Available online at www.sciencedirect.com
SCIENCE DIRECT
Planetary and Space Science 53 (2005) 169–179
Planetary and Space Science
www.elsevier.com/locate/pss

The development of the magnetospheric substorm and its influence on the magnetopause motion

N.S. Nikolaeva[a,*], V.A. Parkhomov[b], N.L. Borodkova[a], S.I. Klimov[a], M.N. Nozdrachev[a], S.A. Romanov[a], Yu.I. Yermolaev[a]

[a]Space Research Institute, Russian Academy of Sciences, Profsoyuznaya 84/32, 117997 Moscow, Russia
[b]Baykalsky State University of Economy and Law, Irkutsk, Russia

Accepted 12 September 2004
Available online 15 December 2004

Abstract

The time development of the magnetospheric substorm on February 10, 1997 and its influence on motion of low-latitude magnetospheric boundary was studied. The plasma and magnetic data obtained on 4 spacecraft (WIND, Interball-1, Geotail, GOES 8) are compared to measurements at ground based stations. The observations show that the release of energy stored in the magnetotail was initiated by tail current disruption in the near-Earth region and that neutral line formation occurred a few minutes after the tail current disruption. Almost simultaneously with the substorm onset, a series of four rapid magnetopause crossings was observed by the Interball-1 on the evening flank of low-latitude magnetosphere. Some of the possible causes of the observed magnetopause motion, such as variations of the solar wind parameters, the Kelvin–Helmholtz instability and substorm processes are considered in the paper. The fast magnetopause motion is observed almost simultaneously with magnetic field variations in the near-Earth magnetotail and geomagnetic Pi2 pulsations on the ground. The results suggest the possible connection of short-time motion of the magnetospheric boundary with tail current disruption and the substorm current wedge formation.

Keywords: Substorm onset; Current disruption; Neutral line formation; Magnetopause; Magnetopause motion; Geomagnetic Pi2 pulsation

1. Introduction

The magnetospheric substorm is a process of explosive release of energy which was stored inside the magnetotail through the magnetospheric interaction with the solar wind. Two competing hypotheses explain the mechanism responsible for the energy release: (1) tail current disruption, which is observed at distances 5–12 Re from Earth near the interface between regions of stretched and dipolar magnetic configuration (Ohtani et al., 1998, 1999) and (2) reconnection initiated by neutral line formation near Earth; in accordance with experimental data, the near-Earth neutral line (NENL) is formed at distances further down the tail, 20–30 Re (Baker et al., 1996; Nagai et al., 1998; Ohtani et al., 1999).

Two possibilities have been considered to join these two mechanisms into a single process. One possibility is that the tail current disruption occurs first near Earth and is followed by tailward expansion of the disruption region, which sets up a favorable condition for neutral line formation further tailward (Jacquey et al., 1991; Ohtani et al., 1992; Lui, 1991). The second possibility is that the neutral line is formed before a substorm onset, and later the tail current is disrupted closer to Earth. The magnetic field dipolarization in the near-Earth region is explained by the pile up of magnetic flux that is ejected from the neutral line towards Earth (Baker and McPherron, 1990; Hesse and Birn, 1991; Birn and Hesse, 1996; Ohtani et al., 1999).

*Corresponding author.
E-mail address: nnikolae@iki.rssi.ru (N.S. Nikolaeva).

0032-0633/$ - see front matter
doi:10.1016/j.pss.2004.09.042

Sergeev et al. (1995), Shiokawa et al. (1998) and Nagai et al. (1998) report events in which fast plasma flow was observed before the onset of Pi2 pulsations. These authors support the hypothesis that substorms are initiated by neutral line formation before the substorm onset. But the process of continuous magnetic flux transfer cannot explain the intensification of the tail current before dipolarization or the explosive character of substorm manifestation on the ground (Ohtani et al., 1999).

The process of substorm development can influence the boundary of the magnetosphere. The distant, −20 to −70 Re, magnetotail boundary expands slowly in the growth phase of a substorm (for 2 h before the substorm onset) and compresses rapidly in the expansion phase of substorms (within 1 hour after substorm onset) (Maezawa, 1975). Meng (1970) show that the dayside magnetosphere is inflated in quiet conditions (low values of the AE index) and is compressed during the development of polar substorms (high values of the AE index). These works considered the magnetospheric boundary motion during time intervals comparable with the duration of the substorm phase (1–2 h).

Two main problems are considered in this work. First, the cause-and-effect relationship between the processes of tail current disruption in the near-Earth region and neutral line formation in the more distant magnetotail. Second, the possible influence of substorm processes which occur inside the tail (during the short time interval near substorm onset) on the magnetospheric boundary located on the western side of the substorm current wedge, i.e. the magnetopause response to tail current disruption and substorm current wedge formation.

With this purpose, we analyze a sequence of substorm onset associated signatures observed during the substorm on February 10, 1997 from 5–6.10 UT and estimate their influence on the motion of the magnetospheric boundary. Simultaneous measurements of the plasma parameters and magnetic field are obtained from the WIND, Interball-1, Geotail, and GOES 8 spacecraft and from the CANOPUS chain of ground based observing stations.

The substorm we study is one of several which were observed on February 10, 1997.

2. Observations

2.1. Localization of spacecrafts

Fig. 1 shows two projections of the location of three spacecraft in the GSM coordinate system for the time interval 5–6.10 UT on February 10, 1997. The solid and dotted lines show the average magnetopause position and Earth's bow shock location according to the Shue et al. (1998) and Fairfield (1971) models. The WIND satellite was in the solar wind 199 Re upstream of Earth. (Xgse = 199 Re, Ygse = 3 Re, Zgse = −17 Re).

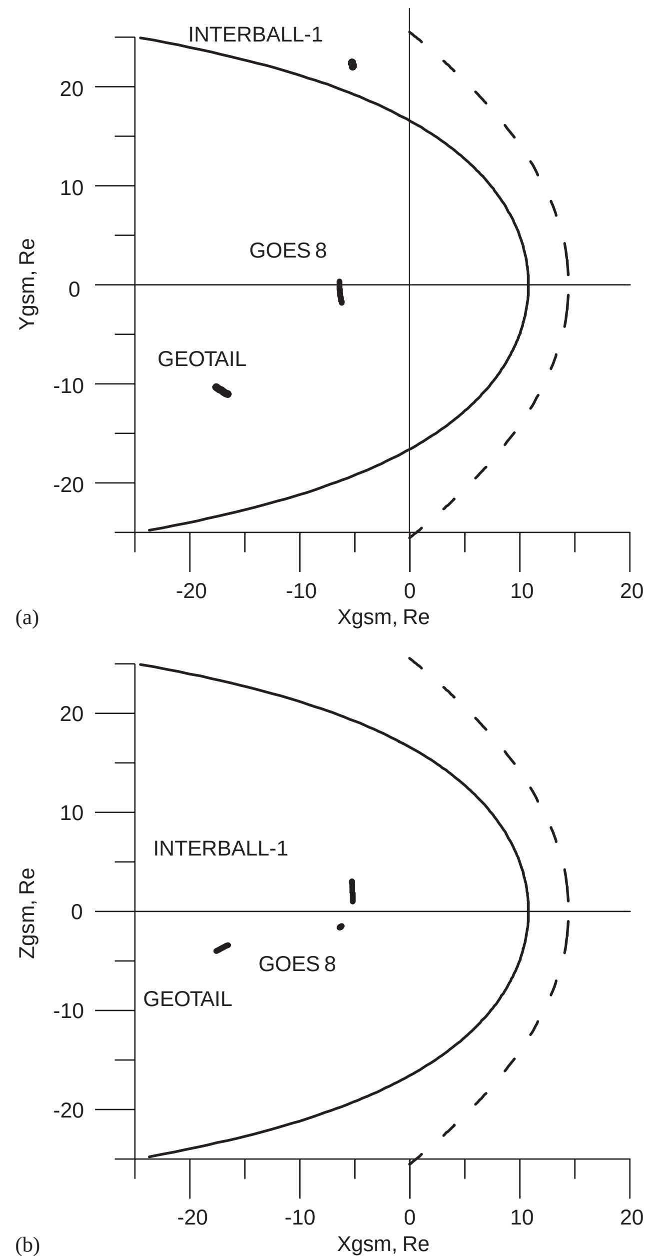

Fig. 1. Spatial localizations of Interball-1, GOES 8, Geotail (a) in equatorial (XY) and (b) meridional (XZ) planes of the GSM coordinate system.

The Interball-1 satellite enters the magnetosphere on the dusk flank at $X\sim-5.2$ Re and moves along the low latitude magnetospheric boundary. The geosynchronous GOES 8 satellite is located at $X\sim-6.4$ Re near the midnight meridian, where dipolarization of the magnetic field is usually observed.

The Geotail satellite is in the magnetotail where neutral lines may form (Ieda et al., 1998), $X\sim-17$ Re, and almost in the middle of the plasma sheet ($|Y|<12$ Re).

2.2. Measurements from ground stations CANOPUS

At the onset of auroral substorms (initiation of the explosive substorm expansion process) many substorm associated features are observed: auroral breakups, Pi2 geomagnetic pulsations, and sharp decreases in magnetic negative bays at high latitudes (Liou et al., 1999). In this paper, the substorm onset was determined from ground based observations. The magnetometer data and optical observations (the ground based all-sky camera and Zenit photometers), combined with cosmic noise absorption data in the auroral zone measured by ground stations located close to magnetic midnight, are used to determine the time $T0$ of substorm onset (Yumoto et al., 1990).

The CANOPUS chain of ground stations was in the premidnight sector of the polar ionosphere (geomagnetic local time MLT = 23–23.5 h). The invariant coordinates of stations vary from $L = 4.25$, ILAT = 60.98 (the most equatorial, PIN) up to $L = 29.96$, ILAT = 79.47 (the most polar station, TAL).

Fig. 2 shows the horizontal H and vertical Z magnetic field components measured by the CANOPUS chain of ground stations. The horizontal H component is designated by the thick line (the axis on the left), the vertical Z component of the magnetic field is designated by the thin line (the axis on the right). The vertical dashed line specifies a substorm onset (the moment $T0$). The geomagnetic field data from the CANOPUS stations show a typical pattern (negative bay) for a substorm in the H component of magnetograms.

The data show that a strong decrease of 200 nT of the horizontal component of the ground magnetic field is observed first (at about 5.27 UT) at Gillam station (station GIL, ILAT = 67.20, $L = 6.66$) signifying the presence of a westward electrojet in the ionosphere. As the substorm evolved, the auroral electrojet expanded westward, poleward and eastward.

We note that the substorm onset obtained from the timing of the negative bay at the Gillam ground station (5.27 UT) is delayed by 2 min from the substorm onset time determined from other signatures (auroral breakup, cosmic noise absorption, and Pi2 pulsations). This discrepancy in timing is attributed to the temporal and spatial limitations of each observational technique used for determination of substorm onset (Liou et al., 1999). In some substorm events, the arrival of the high latitude magnetic bay can be delayed up to tens of minutes even if the high latitude auroral zone geomagnetic observatory is located in the midnight sector (Liou et al., 1999). Here we use optical observations and Pi2 pulsations as indicators of substorm onset (Liou et al., 1999). We suggest that the accuracy of the identification of substorm onset by Pi2 pulsations is within 5 s.

Analysis of ground based magnetometer data shows that the substorm onset was initiated at the latitude of Gillam (GIL) station, then the auroral arc, the electrojet and the source of pulsations are displaced to the north (CHU station). The drift velocity of the source is of order 1°/min, in accordance with previous estimates from auroral arcs observations on Earth and satellites.

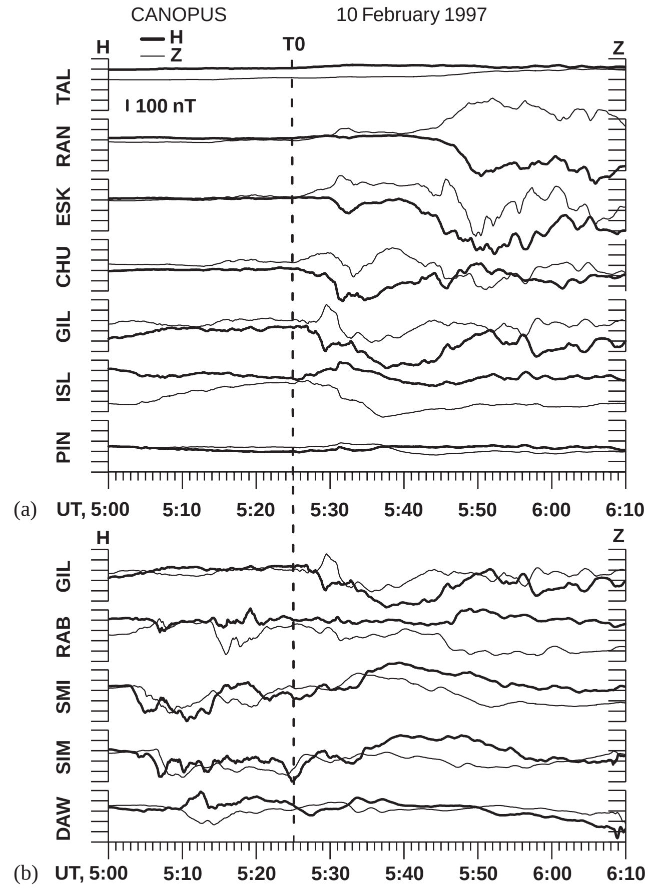

Fig. 2. The H (thick lines) and Z (thin lines) components of the magnetic field measured at CANOPUS ground stations (a) along a meridional chain of stations from the most poleward station of TAL up to the most equatorial of PIN; (b) along a low-latitude chain of stations stretched in the east–west direction from GIL to DAW.

The intensification of the westward auroral electrojet in the midnight sector of the oval is a ground signature of the substorm current wedge formed as a result of the tail current disruption in the near Earth region and its connection inside the ionosphere.

2.3. Measurements in the solar wind

The solar wind plasma and magnetic field data from 5.00 to 6.10 UT on February 10 1997 measured by WIND (Lepping et al., 1995; Ogilvie et al., 1995). The solar wind plasma and interplanetary magnetic field data are presented in Fig. 3; we show (a) the dynamic pressure of solar wind plasma, Pd; (b) the solar wind plasma density, N; (c) solar wind plasma velocity, $|V|$;

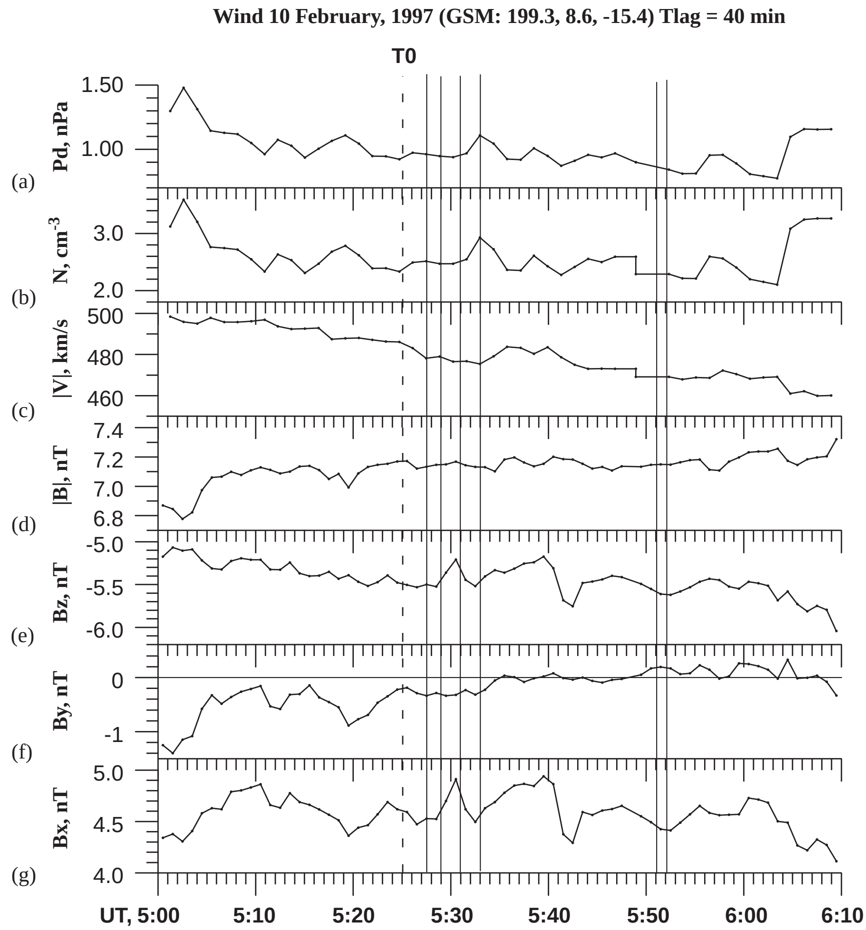

Fig. 3. Solar wind plasma and interplanetary magnetic field data: (a) dynamic pressure Pd, (b) plasma density N, (c) speed of solar wind plasma $|V|$, (d) the magnitude $|B|$ and components (e) Bz, (f) By and (g) Bx of the interplanetary magnetic field.

(d) the magnitude of the interplanetary magnetic field, $|B|$; (e), (f), (g) Bz, By, Bx components of the interplanetary magnetic field, respectively. The vertical dotted line shows the time $T0$ of substorm onset. The solid vertical lines show the magnetopause crossings of the Interball-1 satellite. The time scale is shifted by 40 min to account for the propagation time of the solar wind from WIND to Interball-1.

The solar wind plasma dynamic pressure varies insignificantly and approximately equals to Pd $\sim$ 1 nPa, except near 5.03 UT and 6.03 UT where it increases to 1.5 and 1.3 nPa, respectively. The interplanetary magnetic field strength $|B|$ increases from 6.8 nT at 5.03 UT and then varies about the value $|B| \sim 7.1$–7.4 nT. The interplanetary magnetic field is southward ($Bz \sim -5.5$ nT) and sunward ($Bx \sim 4.5$ nT). The solar wind has a high speed (500 km/s) and low density (2–3.5 cm^{-3}). So, this period is characterized by continuous external driving similar to that described by (Yermolaev et al., 1999). The hourly value of the equatorial D_{st} index reached -45 nT.

2.4. Magnetopause and magnetotail measurements

Fig. 4 shows plasma and magnetic field data; from top to bottom are Interball-1 (a–e), GOES 8 (f–h), and Geotail (i–n) data. The thin vertical lines on panels (a)–(e) mark the times of the multiple magnetopause crossings. $T1$ shows the time of the first magnetopause crossing by Interball-1. In Fig. 4e, arrows directed upward (downward) signal the entry into (exit from) the magnetosphere. The thin vertical lines in panels (f)–(h) show the time interval of the magnetic field variations. The line $T2$ shows the start of the magnetic field dipolarization. The vertical lines in Fig. 5(i–n) are labeled $T3(1)$, the instant of a neutral line formation and $T3(2)$, the start of the magnetic flux transfer toward Earth.

The plasma ion temperature, Ti, density, Ni, and velocity, Vi are obtained by the Interball-1 CORALL instrument and have a 2-min resolution (Yermolaev et al., 1997). The integral flux of plasma Fi was measured by the VDP instrument with a time resolution of 1 s (Safrankova et al., 1997). The magnetic field

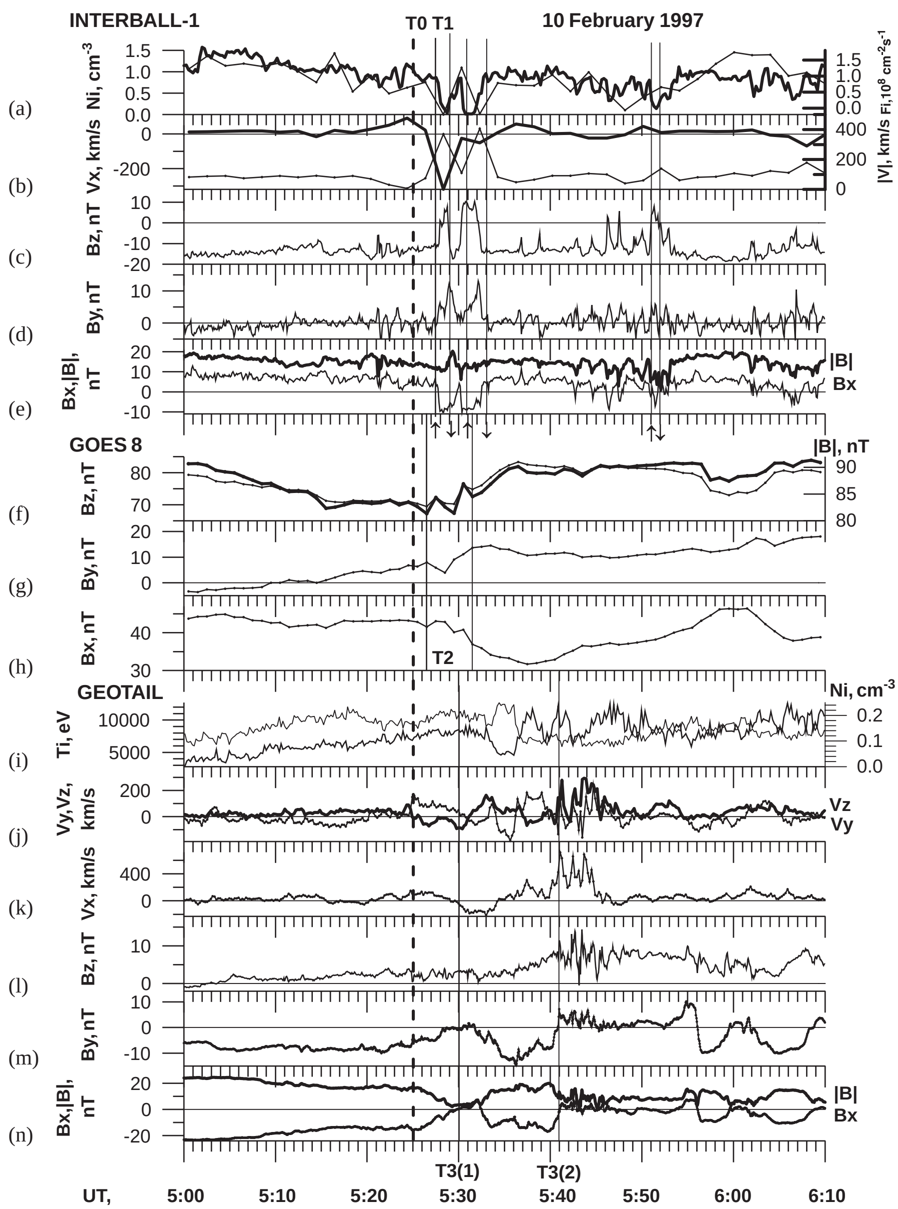

Fig. 4. The plasma and magnetic field data measured by Interball-1: (a) density of plasma ions Ni (thin line, left scale) and integrated flux of plasma Fi (thick line, right scale); (b) Vx component of plasma velocity (thin line, left scale) and $|V|$ the plasma bulk speed (thick line, right scale); (c) Bz, (d) By and (e) Bx (thin line) components and $|B|$ (thick line) of the magnetic field. The GOES 8 data: (f) Bz component (thin line, left scale) and magnitude $|B|$ (thick line, right scale) of the magnetic field; (g) By, (h) Bx components of the magnetic field. The Geotail data: (i) ion plasma density Ni (thin line, right scale) and temperature Ti (thick line, left scale); (j) Vy (thin line) and Vz (thick line) components of plasma velocity; (k) Vx component of plasma velocity; (l) Bz; (m) By; (n) Bx (thin line) components and $|B|$ (thick line) of the magnetic field.

data (the MIF-M, FM-3 instruments) are averaged over 6-s (Klimov et al., 1997). The plasma electron data are obtained with the ELECTRON instrument (Sauvaud et al., 1997). The magnetic field data obtained by the GOES 8 satellite are 1-min averages. On the Geotail satellite, the plasma parameters have 12-s resolution and the magnetic field data have 3 s resolution (Kokubun et al., 1994; Mukai et al., 1994).

Interball-1 was inside the magnetosheath (MSH) except for a few intervals (marked by upward arrows in Fig. 4e) when the satellite briefly entered the magnetosphere (MSP). At the boundary the plasma density decreases from 1 to 1.5 cm^{-3} (inside MSH) to near 0.1 cm^{-3} (inside MSP), the plasma temperature increases from 100 to 200 eV (inside MSH) to 1–2 keV (inside MSP). The sharp change of the electron spectra and occurrence of electrons with energies of several keV signals an entry into the plasma sheet.

As shown by Fig. 4(a–e), the first magnetopause crossing by Interball-1 (T1, to MSP from MSH) was at

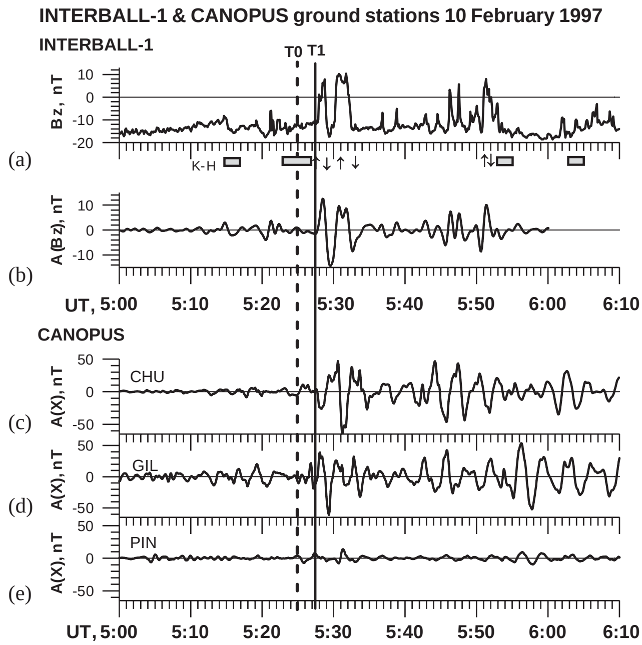

Fig. 5. (a) *Bz* component measured by Interball-1, (b) amplitude of variation of *Bz* filtered in a range of frequencies of Pi2 pulsations; (c, d, e) filtered amplitudes of variations of horizontal components at CHU, GIL, PIN ground stations, accordingly.

5.27.30 UT, 2.5 min after the substorm onset. The motion of the magnetospheric boundary is quasi-periodic with a period of about ~ 80 s (4 magnetopause crossings in 5.5 min). The times of the magnetopause crossings were based on the plasma and magnetic field data and have an accuracy of approximately 10 s.

Fig. 4(f–h) shows that the magnetic field lines observed by GOES 8 in the near-Earth tail are stretched (*Bz* component is small) until *T*2 at 5.26.30 UT. The stretching of magnetic field lines in the tail direction was associated with a thinning of the plasma sheet and intensification of the tail current. The magnetic field fluctuations are observed from 5.26.30 to 5.31.30 UT. The configuration of the magnetic field varies and becomes more dipole-like (*Bz* component increase with simultaneous decrease of *Bx*). A change of the magnetic field configuration in the near-Earth tail region occurs during the time interval 5.26.30–5.31.30 UT (solid vertical lines, Fig. 4(f–h)). We suggest that dipolarization of magnetic field starts at that time.

Fluctuations of the magnetic field during the magnetic field dipolarization in the near tail were associated either with thin filamentary structure in the tail current sheet during disruption or with an oscillation of the substorm current wedge formed at the time of the current disruption (Lester et al., 1989; Lopez and Lui, 1990; Lui, 1996). The character of the variation of *Bz* observed on GOES 8 is similar to that of the *Bz* variation observed on Interball-1; the periods of fluctuations (1–2 min) are similar. Thus, the disruption of the tail current sheet (magnetic field dipolarization) and oscillatory motion of the magnetopause were observed almost simultaneously, and had close temporal fluctuation scales.

The plasma parameters and magnetic field profiles measured in the middle tail region (Geotail) show that the satellite was located inside the plasma sheet (Fig. 4i–n). The velocity $Vx \sim 200\,\mathrm{km/s}$ of the plasma flow directed towards Earth began to increase at ~ 5.22 UT, before the ground indication of substorm onset, and it remained high at the time of substorm onset. However, magnetic field was directed toward Earth, hence the plasma moved along the magnetic field and did not transfer magnetic flux toward Earth and thus did not influence the magnetic field observed by GOES 8. At this time Geotail was probably located in the external plasma sheet or plasma sheet boundary layer (PSBL). In this region the plasma flow, directed toward Earth, propagates along the magnetic field (Baumjohann et al., 1990).

At ~ 5.30 UT the direction of the fast plasma flow changes and plasma moves with velocity $Vx \sim -200\,\mathrm{km/s}$ tailward. The onset of the fast tailward plasma flow gives evidence that the near Earth neutral line (NENL) was formed not later than 5.30 UT (at *T*3(1) in Fig. 4(i–n)) Earthward of Geotail (Angeloupoulos et al., 1992). After 5.35 UT the plasma flow turns Earthward and *Vx* increases to ~ 600 km/s at 5.41 UT.

The source of the fast velocity plasma flow from 5.30 to 5.45 UT may be a neutral line formed not later than at 5.30 UT. When the plasma flow moves toward Earth the direction of its propagation direction relative to the magnetic field varies. From 5.34 to 5.41 UT the plasma flow is Earthward along the magnetic field (*Bx* is the main component of the magnetic field). At 5.41 UT, the plasma starts to move Earthward with a maximum velocity $Vx = \sim 600\,\mathrm{km/s}$ across the magnetic field direction (*Bz* is the main component of the magnetic field). So the plasma flow transfers magnetic flux, which may influence the configuration of the magnetic field near Earth, but only after the substorm onset and magnetic field dipolarization observed by GOES 8.

The magnetic field variations measured by Interball-1 at the magnetosphere boundary and the short-time variations of the magnetic field measured by ground stations close to substorm onset are observed almost simultaneously and have similar periods of fluctuation.

Fig. 5 shows from top to bottom: (a) *Bz* measured by Interball-1; (b) the amplitude of the variation of *Bz* filtered in a range of frequencies appropriate to the periods of the Pi2 pulsations (40–150 s); (c), (d), (e) amplitudes of fluctuations of the horizontal (*X*) magnetic field component at ground stations Fort Churchill (CHU), Gillam (CIL), and Pinawa (PIN), filtered in a range of the frequencies characteristic for Pi2 of pulsations. The vertical dotted line shows the substorm onset time $T0$. The solid vertical line show $T1$, the first magnetopause crossing by Interball-1. In Fig. 5a the upward (downward) arrows correspond to entrance into (exit from) the magnetosphere. The rectangles in the top panel mark intervals of time when the K–H instability is excited.

The similar behavior of the filtered components of magnetic field on Interball-1 and on Earth is seen in Fig. 5. The correlation coefficient between the filtered amplitudes of variation for the horizontal component at ground station Gillam and for the Bz magnetic field component on Interball-1 reaches $K = 0.67$. This result could be a random coincidence between two different independent phenomena; a larger statistical base of events is needed. However, this result suggests that the short-term magnetopause motion correlates with the geomagnetic Pi2 pulsations which indicate a substorm onset.

3. Discussion of results

3.1. Temporary sequence of substorm development

The temporal sequence of the basic substorm signatures observed on the ground as well as on Interball-1, GOES 8, and GEOTAIL was summarized in Table 1. Table 1 shows that the magnetic field dipolarization in the near-Earth magnetotail is observed 1.5 min after substorm onset and that the neutral line formation occurs 5 min after substorm onset as determined from the ground based data.

If pile up of magnetic flux near Earth causes the observed magnetic field dipolarization, a definite time sequence of substorm features is predicted, in particular that the NENL formation and the magnetic flux transfer to Earth should be observed earlier than the onset of magnetic field dipolarization. The fast plasma flow from the NENL should move not only toward Earth but also across the magnetic field. Such a plasma flow accelerated in the NENL is observed at 5.41 UT, much later than start of the magnetic field dipolarization at 5.26.30 UT.

However, we must discuss the accuracy of the timing of substorm NENL formation and tail current disruption (dipolarization). The accuracy of determination of these times is restricted by the time resolution of the data sets: 1 min for dipolarization onset and 12 s for the neutral line formation. The time of the neutral line formation in the tail has an additional uncertainty connected with the location of the Geotail satellite relative to the middle of the tail. Since Geotail is on the morning side (MLT $\sim$ 3 h), the neutral line formation in

Table 1
A temporary sequence of events during substorm on February 10, 1997

Time, UT	Object	Observation	Interpretation
$T0 = 5.25.00$	Ground based data	Onset of Pi2 pulsations, the auroral arc reach the most southern position, the sudden brightening of equatorial arc near the magnetic midnight, beginning of cosmic noise absorption	Onset of substorm expansion process
$T2 = 5.26.30$	GOES 8	The growth of Bz and reduction of Bx components, magnetic field fluctuations are beginning	Onset of magnetic field dipolarization (tail current disruption), the substorm current wedge formation
5.26.30–5.31.30	GOES 8	Magnetic field fluctuations near the Earth with duration 5 min	Filamentary current structure? Oscillation of substorm current wedge?
$T1 = 5.27.30$	Interball-1	The first magnetopause crossing, the first entry in magnetosphere (MSP) from magnetosheath (MSH)	Expansion of MSP before onset
5.27.30–5.33.00	Interball-1	Multiple magnetopause crossings, 4 crossings for 5.5 min	The short time magnetopause motion (period 80 s); oscillation of substorm current wedge?
$T3(1) = 5.30.00$	Geotail	The start of a fast velocity plasma flow in tailward direction	Near the Earth neutral line (NENL) formation not later than 5.30 UT on Earth's side from Geotail
5.30.00–5.45.00	Geotail	Fast velocity plasma flow in various direction relative magnetic field	The time interval of observation of fast plasma flow accelerated by a neutral line
$T3(2) = 5.41.00$	Geotail	Plasma flow with most fast velocity 600 km/s, which moved across a magnetic field towards the Earth	Start of magnetic flux transferring toward the Earth
5.41.00–5.45.00	Geotail	The time interval (4 min) during which a fast velocity plasma flow is moving to the Earth across a magnetic field	The magnetic flux transferring from NENL towards the Earth

the middle of the tail could take place 5.5 min earlier if the propagation speed of the neutral line is $\sim 200\,km/s$ (see Vy in Fig. 4(j)). In addition, the fluctuations of the magnetic field observed at the beginning of dipolarization can influence the accuracy of the determination of the dipolarization onset $T2$.

The uncertainty in the determination of the dipolarization onset $T2$ due to magnetic field fluctuations and neutral line formation associated with projection of Geotail data to the ionosphere can be 5–5.5 min. However, even in this worst case, the fast plasma flow ejected from the NENL and the transferred magnetic flux at the GOES 8 position would be observed 4.5–11 min after dipolarization.

The analysis of this substorm event shows that magnetic field dipolarization observed near Earth may not be a consequence of pile up of magnetic flux ejected from the neutral line toward Earth. In a substorm we might have two independent phenomena—NENL formation and current disruption, or dependent phenomena with a current disruption which expanded tailward and pushed the neutral line tailward (Jacquey et al., 1991; Ohtani et al., 1992, 1998). Current sheet disruption could be an independent process, caused by an MHD instability or local current instability (Lui et al., 1991; Roux et al., 1991; Ohtani et al., 1999).

3.2. The magnetopause motion during substorm

The second problem addressed by this paper is the substorm influence on small period ($\sim 80\,s$) motions of the magnetospheric boundary. What is the cause of short-time-period magnetopause motions observed by Interball-1?

Our results differ from previous work; Meng (1970) found a relationship between the occurrence of polar substorms and the magnetospheric size. He concluded that the dayside magnetosphere is compressed when polar substorms are in progress. Maezawa (1975) found that within 2 h of substorm onset the radius of the magnetotail increases and during the 1 h after substorm onset the size of the tail decreases. In both of these studies the behavior of the magnetospheric boundary over long time intervals, 1–2 h, was analyzed.

Meng (1970) examined the subsolar region (MLT $\sim$ 11–13 h) magnetopause motion dependence on substorm activity as determined by the magnitude of one-hour averaged values of the AE index of auroral activity. However, AE index is not a precise indicator of polar substorms along a contracted oval, and is not reliable for determination of the substorm onset time. For example, the AE index may be as low as 20 nT during a contracted oval substorm and may be as high as 50 nT during quiet conditions (Lui et al., 1975). Meng (1970) shows that in quiet conditions (low values of AE index) the dayside magnetosphere distends, but when polar substorms develop (at high values of AE index), the dayside magnetosphere contracts.

Maezawa (1975) study the boundary motion of the distant magnetotail (from -20 to $-70\,Re$) during substorms, in particular the motions of the magnetopause within a few hours of substorm onset. The onset of the substorm expansion phase was defined as the onset time of the low latitude positive bay observed near the midnight meridian. The magnetopause crossings were identified by sudden changes in the magnetic field. Ten-minute averages of the data were used. Of the roughly 40 magnetopause boundary crossings, almost all occurred more than 20 min after substorm onset. No magnetotail boundary crossings occurred close to the time of substorm onset. The behavior of the magnetospheric boundary very close to the time of substorm onset was not considered in these works (Meng, 1970; Maezawa, 1975).

Thus the result of our study differs from Meng (1970) and Maezawa (1975) because we investigate a different region of the magnetotail and determine the substorm onset with more accuracy.

Due to the high time resolution of the instruments used for identification of the magnetopause position, the multiple crossings of the magnetospheric boundary were measured by Interball-1 very close to the time of substorm onset. In addition, Interball-1 passes across the magnetospheric boundary near-Earth region at low latitudes (on the western side of the substorm current wedge). This location allows us to study possible connection of short-time magnetopause motions with processes of current disruption (dipolarization) and substorm current wedge formation.

Causes of magnetopause boundary motion include changing solar wind conditions (plasma dynamic pressure and Bz component of interplanetary magnetic field), the variation of plasma pressure inside the magnetosheath, processes of local magnetic field reconnection and the Kelvin–Helmholtz (K–H) instability.

We consider two sources of the magnetopause motion: variations of the solar wind and the K–H instability. Fig. 3 shows that the solar wind variations are insignificant during the magnetopause crossings. The interplanetary magnetic field has a large southerly component, $Bz = -5.5\,nT$.

The influence of variations in solar wind parameters on the magnetopause location can be estimated using the Sh98 model (Shue et al., 1998). This empirical model (Shue et al., 1998) predicts the magnetopause position based on the dynamic pressure of the solar wind plasma and the Bz component of the interplanetary magnetic field. We suggest that some discrepancies between the observed magnetopause position and those predicted by the model Sh98 (Shue et al., 1998) may be due to internal causes (for example, substorm development). The solar wind data from Wind were used as input parameters for the model. The time delay (40 min) due to solar wind propagation from Wind to Interball-1 was taken into account. The Sh98 model predicts that the Interball-1 satellite is outside the magnetospheric boundary (inside the magnetosheath) by about 2 Re. The observed variations of solar wind parameters do not explain the observation of multiple magnetopause crossings by Interball-1 in time interval close to substorm onset.

Another source of magnetopause motion is the *K–H* instability. The condition for instability at the boundary is the inequality (1) in which wave growth results when the centrifugal force due to curvature in flow streamlines (excited *K–H* force, left part of (1)) exceeds the increase in magnetic tension due to bending of magnetic field lines (stabilizing *K–H* force, right part (1)) (Kivelson and Chen, 1995). The given inequality is valid assuming the ideal MHD approximation and incompressible plasma:

$$m_p\left[\frac{n_1 n_2}{n_1+n_2}\right](\vec{k}\Delta\vec{V})^2 > \frac{1}{\mu_0}[(\vec{k}\vec{B}_1)^2+(\vec{k}\vec{B}_2)^2], \qquad (1)$$

where m_p is the mass of proton, μ_0 the magnetic permeability, $\vec{k}$ the unit vector in a direction of wave propagation, $\Delta\vec{V}=\vec{V}_1-\vec{V}_2$ the vector difference of plasma velocity in the region 1 (internal region MSP) and 2 (external region MSH), accordingly; $\vec{B}_1, n_1$ and $\vec{B}_2, n_2$ are the vectors of the magnetic field and plasma density on internal and external sides.

In the formula (1) the right and left sides both have the scalar products of vectors $\vec{k}$, $\vec{B}_1$, $\vec{B}_2$ and $\Delta\vec{V}$. The measured plasma parameters $\vec{V}_1$, n_1, $\vec{V}_2$, n_2 and magnetic field vectors $\vec{B}_1$, $\vec{B}_2$ from Interball-1 were used as input data for the *KH* relation (1). The criterion (1) for *K–H* instability excitation was checked for the time interval 5.00–6.10 UT for various directions of the vector $\vec{k}$. In the time intervals marked by grey rectangles in Fig. 5b, the conditions for excitation of the *K–H* instability are met if wave propagation is along the Ygsm axis.

Thus the *K–H* instability is excited before the magnetopause motion, but is damped during the magnetopause motion (see Fig. 5b). We note that (Miura, 1995) show that northerly IMF is more favorable for excitation of the *K–H* instability and that the *K–H* instability quickly damps for southward IMF (as in our event).

Detailed comparison of observations from GOES 8 and Interball-1 with magnetometer measurements at the CANOPUS stations (Figs. 2 and 4) gives two major results. First, three different events which were observed in different areas of the magnetosphere (the magnetopause motion, the magnetic field dipolarization in the near tail, and geomagnetic Pi2 pulsation) occurred successively during a short interval of time, $\sim$2.5 min. Second, the period of variations of magnetic field components on Interball-1 was close to the period of variations in the magnetic field on GOES 8 during dipolarization and to variations in the geomagnetic field on Earth (this period corresponds to that of Pi2 pulsations).

Thus, three different phenomena are observed with a small delay in the three different spatial regions. Two of them (the magnetic field variations during the current disruption and Pi2 pulsations) are usually explained by fluctuation of the substorm current wedge. The short-time magnetopause motion could also be connected with the substorm current wedge.

The Pi2 pulsations may be initiated by tail current disruption and are Alfvenic waves which transfer field-aligned currents. These currents are part of the substorm current system, and are included in the substorm current wedge (Lysak and Dum, 1983; Southwood and Hughes, 1985). The Pi2 pulsations are caused by a partial reflection of the field-aligned current from the ionosphere (Lysak and Dum, 1983). The 100 s period of Pi2 results from the time required for a wave to pass from the equator to the ionosphere and back to the equator. The variation of the *Bz* component observed on Interball-1, and also the magnetic field fluctuations on GOES 8, are likely to be associated with intensity changes of the cross-tail current which is part of substorm current system.

Two possible connections between the magnetopause motions and Pi2 pulsations are offered. The oscillation of the substorm current wedge could cause these events. The substorm wedge oscillation may produce magnetic field fluctuations in the region of tail current disruption (filamentary structure of current), geomagnetic Pi2 pulsations on Earth (field-aligned current), and the magnetopause boundary motion on the western side of the substorm current system (Lester et al., 1989; Lopez and Lui, 1990). Also, we cannot exclude the possibility that in this substorm event direct connection of the substorm current wedge with the magnetopause occurred due to the large increase of auroral and field-aligned currents and strong curvature of the magnetic field lines. In any case, the idea of coupling the substorm current wedge to magnetopause oscillations merits subsequent study.

Thus the magnetospheric boundary, as the part of substorm current system, experiences rapid motion during tail current disruption. Our results allow us to suggest possible connection of the observed magnetopause motion with current disruption and substorm current wedge formation.

4. Conclusion

We analyze substorm associated signatures observed on February 10, 1997 by four spacecraft and by ground based monitors. Wind was in the solar wind, Interball-1 crosses the magnetospheric boundary, GOES 8 was located near Earth's magnetotail, and Geotail was in the more distant magnetotail. The high latitude meridional chain of ground stations CANOPUS was located in the midnight sector of the auroral zone. The interplanetary magnetic field was southward during the study period. Substorm onset was determined from ground based data including all sky camera data, cosmic noise absorption, and geomagnetic Pi2 pulsations. The following results were obtained:

1. The onset of a substorm begins with current disruption in the near-Earth region. First magnetic field dipolarization is observed. Neutral line formation occurs several minutes after the onset of the current disruption. In the substorm event, the neutral line formation and Earthward magnetic flux transfer cannot explain the magnetic field dipolarization near Earth observed by GOES 8. A fast-velocity plasma flow, which transfers magnetic flux toward Earth and can influence on the configuration of the magnetic field near Earth, is detected later (16 min after substorm onset).

2. Multiple magnetopause crossings are observed almost simultaneously with substorm onset (Pi2 pulsations) and tail current disruption (magnetic field dipolarization). The time period of the magnetospheric boundary motion ($\sim$ 80 s) is close to the time period of the Pi2 pulsations (40–150 s). A correlation coefficient of 0.67 is obtained between the amplitude of Pi2 pulsations at station Gillam and the filtered (in the same frequency range as Pi2 pulsation) amplitude of variations of the magnetic field measured during the transition through the magnetospheric boundary.

3. The observed multiple magnetopause crossings cannot be explained by the variation of the solar wind parameters. The measurements on WIND show that the solar wind parameters vary insignificantly. The empirical Sh98 model predicts that the magnetospheric boundary is located approximately on $\sim$ 2 Re closer to Earth than observed. The criterion for Kelvin–Helmholtz instability excitation performed under the MHD approximation suggests that the plasma is *K–H* unstable but is possibly damped by the magnetopause motion.

4. We suggest a possible connection of short-time magnetopause motions with tail current disruption and substorm current wedge formation.

Acknowledgements

The authors thank A. Lazarus and P. Lepping for presiding on the solar wind data and interplanetary magnetic field received on the WIND probe, Mukai and Kokubun for the plasma and magnetic data obtained on the Geotail satellite, H. Singer for the data on the magnetic field measured on the GOES 8 spacecraft, and also the Canadian Space Agency for program CANOPUS with ground magnetometer data. We express deep gratitude to G. Zastenker and V. Mishin for discussion of results. The work was supported by the grants RFFI N01-02-16182, N01-05-64203, N02-02-17160 and N04-02-16131, and IN-TAS N03-51-3738.

References

Angeloupoulos, V., Kennel, C.F., Coroniti, F.V., Pellat, R., Kivelson, M.G., Walker, R.J., Baumjohann, W., Paschmann, G., Luhr, H., 1992. Bursty bulk flows in the inner central plasma sheet. J. Geophys. Res. 97, 4027.

Baker, D.H., McPherron, R.L., 1990. Extreme energetic particle decreases near geostationary orbit: a manifestation of current diversion within the inner plasma sheet. J. Geophys. Res. 101, 6591.

Baker, D.N., Pulkkinen, T.I., Angelopoulos, V., Baumjohann, W., McPherron, R.L., 1996. Neutral line model of substorms: past results and present view. J. Geophys. Res. 101, 12975.

Baumjohann, W., Paschmann, G., Luhr, H., 1990. Characteristics of the high-speed ion flows in the plasma sheet. J. Geophys. Res. 95, 3801.

Birn, J., Hesse, M., 1996. Details of current disruption and diversion in simulations of magnetotail dynamics. J. Geophys. Res. 101, 15345.

Fairfield, D., 1971. Average and unusual locations of the Earth's magnetopause and bow shock. J. Geophys. Res. 76, 6700.

Hesse, M., Birn, J., 1991. On dipolarization and its relation to the substorm current wedge. J. Geophys. Res. 96, 19417.

Ieda, A., Machida, S., Mukai, T., Saito, Y., Yamamoto, T., Nishida, A., Terasawa, T., Kokubun, S., 1998. Statistical analysis of the plasmoid evolution with Geotail observations. J. Geophys. Res. 103, 4453.

Jacquey, C., Sauvaud, J.-A., Dandouras, J., 1991. Location and propagation of the magnetotail current disruption during substorm expansion: analysis and simulation of an ISEE multi-onset event. Geophys. Res. Lett. 18, 389.

Kivelson, M.G., Chen, S.-H., 1995. The magnetopause: surface waves and instabilities and their possible dynamical consequences. In: Physics of the Magnetopause. AGU Geophysical Monograph, vol. 90, pp. 257.

Klimov, S.I., et al., 1997. ASPI experiment: measurements of fields and waves onboard the Interball-1 spacecraft. Ann. Geophys. 15, 514.

Kokubun, S., Yamamoto, T., Acuna, M.H., Hayashi, K., Shiokawa, K., Kawano, H., 1994. The Geotail magnetic field experiment. J. Geomagn. Geoelectr. 46, 7.

Lepping, R.P., Acuna, M.H., Burlaga, L.F., et al., 1995. The WIND magnetic field investigation. In: Russell, C.T. (Ed.), The Global Geospace Mission. Kluwer Academic Publishers, Dordrecht, p. 207.

Lester, M.H., Singer, J., Smith, D.P., Hughs, W.J., 1989. Pi2 pulsations and the substrom current wedge: low latitude polarization. J. Geophys. Res. 94, 17133.

Liou, K., Meng, C.-I., Lui, T.Y., et al., 1999. On relative timing in substorm onset signatures. J. Geophys. Res. 104, 22807.

Lopez, R.E., Lui, A.T.Y., 1990. A multi-satellite case study of the expansion of a substorm current wedge in the near Earth magnetotail. J. Geophys. Res. 95, 8009.

Lui, A.T.Y., 1991. A synthesis of magnetospheric substorm models. J. Geophys. Res. 96, 1849.

Lui, A.T.Y., 1996. Current disruption in the Earth's magnetosphere: observations and models. J. Geophys. Res. 101, 13067.

Lui, A.T.Y., Anger, C.D., Akasofu, S.-I., 1975. The equatorward boundary of the diffuse aurora and auroral substorms as seen by the Isis2 auroral scanning fotometer. J. Geophys. Res. 80, 3603.

Lui, A.T.Y., Chang, C.L., Mankofsky, A., Wong, H.K., Winske, D., 1991. A cross-field current instability for substorm expansions. J. Geophys. Res. 96, 11389.

Lysak, R.E., Dum, C.T., 1983. Dynamics of magnetosphere–ionosphere coupling including turbulent transport. J. Geophys. Res. 88, 365.

Maezawa, K., 1975. Magnetotail boundary motion associated with magnetospheric substorm. J. Geophys. Res. 80, 3543.

Meng, C.I., 1970. Variation of the magnetopause position with substorm activity. J. Geophys. Res. 75, 3252.

Miura, A., 1995. Kelvin–Helmholtz instability at the magnetopause: computer simulations. In: Physics of the Magnetopause. AGU Geophysics Monograph, vol. 90, pp. 285.

Mukai, T., et al., 1994. The low energy particle (LEP) experiment onboard the Geotail satellite. J. Geomagn. Geoelectr. 46, 669.

Nagai, T., Fuijimoto, M., Saito, Y., Machida, S., Terasawa, T., Nakamura, R., Yamamoto, T., Mukai, T., Nishida, A., Kokubun, S., 1998. Structure and dynamics of magnetic reconnection for substorm onsets with Geotail observations. J. Geophys. Res. 103, 4419.

Ogilvie, K.W., Chornay, D.J., Fritzenreiter, R.Y., et al., 1995. A comprehensive plasma instrument for the WIND spacecraft. In: Russell, C.T. (Ed.), The Global Space Mission. Kluwer Academic Publishers, Dordrecht, p. 55.

Ohtani, S., Kokubun, S., Russell, C.T., 1992. Radial expansion of the tail current disruption during substorms: a new approach to the substorm onset region. J. Geophys. Res. 97, 3129.

Ohtani, S., Takahashi, K., Higuchi, T., Lui, A.T.Y., Spence, H.E., 1998. AMPTE/CE—SCATHA simultaneous observations of substorm-associated magnetic fluctuations. J. Geophys. Res. 103, 4671.

Ohtani, S., Creutzberg, F., Mukai, T., Singer, H., Lui, A.T.Y., Nakamura, M., Pricryl, P., Yumoto, K., Rostoker, G., 1999. Substorm onset timing: the December 31, 1995, event. J. Geophys. Res. 104, 22713.

Roux, A., Perraut, S., Robert, P., Morane, A., Pedersen, A., Korth, A., Kremser, G., Aparicio, B., Rodgers, D., Pellinen, R., 1991. Plasma sheet instability to the westward traveling surge. J. Geophys. Res. 96, 17697.

Sauvaud, J.-A., et al., 1997. The Interball-Tail ELECTRON experiment: initial results on the low latitude boundary layer of the dawnside magnetosphere. Ann. Geophys. 15, 514.

Safrankova, J., Zastenker, G., Nemecek, Z., et al., 1997. Small scale observation of the magnetopause motion: preliminary results of the INTERBALL project. Ann. Geophys. 15, 562.

Sergeev, V.A., Angelopoulos, V., Mitchell, D.J., Russell, C.T., 1995. In situ observations magnetotail reconnection prior to the onset of small substorms. J. Geophys. Res. 100, 19121.

Shiokawa, K., Baumjohann, W., Haerendal, G., Paschmann, G., Fennell, J.G., Friis-Christensen, E., Luhr, H., Reeves, G.D., Russell, C.T., Sutcliffe, P.R., Takahashi, K., 1998. High-speed ion flow, substorm current wedge and multiple Pi2 pulsations. J. Geophys. Res. 103, 4491.

Shue, J.-H., Song, P., Russell, C.T., Steinberg, J.T., Chao, J.K., et al., 1998. Magnetopause location under extreme solar wind conditions. J. Geophys. Res. 103, 17691.

Southwood, D.J., Hughes, W.J., 1985. Concerning the structure of Pi2 pulsations. J. Geophys. Res. 90, 386.

Yermolaev, Yu.I., Fedorov, A.O., Vaisberg, O.L., Balebanov, V.M., Obod, Y.A., Himenez, R., Fleites, J., Llera, L., Omelchenko, A.N., 1997. Ion distribution dynamics near the Earths bow shock: first measurements with 2-D ion energy spectrometer CORALL on Interball-1 tail probe satellite. Ann. Geophys. 15, 533.

Yermolaev, Yu.I., Zelenyi, L.M., Borodkova, N.L., Kovrazhkin, R.A., Lutsenko, V.N., Petrukovich, A.A., Savin, S.P., Skalsky, A.A., Sergeev, V.A., Mukai, T., Kokubun, S., Liou, K., Meng, C.-I., Parks, G., Sauvaud, J.-A., 1999. Global substorm effect and convection jet under the conditions of continuous external driving: multi-spacecraft observations on December 22–23, 1996. Czech. J. Phy. 49, 625.

Yumoto, K., et al., 1990. Multiple ground based and satellite observations of global Pi2 magnetic pulsations. J. Geophys. Res. 95, 15175.